Comparison of One-Dimensional and Two-Dimensional Reference Signal Representation for Insulation Aging State Recognition

Mikhail Olkhovskiy, Eva Müllerová, Petr Martínek
Faculty of electrical engineering,
University of West Bohemia,
Pilsen, Czech Republic
mikhail@fel.zcu.cz, mullerov@fel.zcu.cz, petrmart@fel.zcu.cz

2022 International Conference on Diagnostics in Electrical Engineering (Diagnostika) | 978-1-6654-8082-6/22/$31.00 ©2022 IEEE | DOI: 10.1109/Diagnostika55131.2022.9905173

***Abstract*—This paper compares the performance of one–dimensional and two–dimensional convolutional neural networks in the task of analyzing a reference signal while determining the degradation level of single-core polymer-insulated cable. In this work was designed the set of reference signals and several forms of representing of these signals in the form of one-dimensional and two-dimensional tensors. Then, an experimental determination of the most effective version of the reference signal is carried out in terms of classification accuracy and the most effective form of representation of this signal was found, as well as most efficient type of neural network.**

Keywords—one-dimensional neural networks, convolutional networks, reference signal processing, signal analysis, cable insulation, classification accuracy

I. Introduction

The ever–increasing demands on the operation of electrical networks, from an economic point of view, do not allow us just shutdown of electrical equipment in order to perform diagnostics and determine their condition. Efforts to reduce production costs affect a way an insulation system is dimensioned. As a result, an insulation system operates within narrow safety physical limits that are difficult to control. Intelligent online diagnostic and monitoring tools should improve the situation. They are also important in future smart grids, where it would be possible to automatically evaluate a status of equipment and a risk of failure. The current trend is to develop new sophisticated algorithms for data processing and analysis. The modern trend of research area in the field of diagnostics of high–voltage equipment is using of artificial neural networks. There are a large number of neural network algorithms. Each of these algorithms has its own strengths and weaknesses. The most promising type of neural network is convolutional neural networks [1]. They can be divided into types depending on the input data and used network filters kernel. Networks that use two-dimensional kernels in their convolutional layers are very popular. Recently, however, convolutional networks have begun to develop towards using of one-dimensional kernels for processing input data in a time–sequence form. Therefore, the purpose of this research is to compare the effectiveness of these algorithms in the classification of diagnostic signals.

Convolutional neural networks have been replacing previous algorithms since 2012. An example is CERN organization, where "support vector machine" and "decision trees" methods were previously used for data analysis, but are currently being replaced by Keras-based deep neural networks [2]. At the large hadron collider, the data flow from the proton collision detectors reaches such a value that it is not possible to record all the data, so a real-time data filtering mechanism based on the principle of deep learning is applied [3]. The principle of the convolution operation can be described by (1). Where *i, j, k* indicates the positions along the height (*H*), width (*W*), and depth (*D*) of the *p*-th filter in the *q*-th layer.

$$h_{ijp}^{(q+1)} = \sum_{r=1}^{H_q} \sum_{s=1}^{W_q} \sum_{k=1}^{D_q} w_{rsk}^{(p,q)} h_{i+r-1,j+s-1,k}^{(q)} \quad (1)$$

Where:

$h_{ijp}^{(q)}$ – output feature map;

$w_{rsk}^{(p,q)}$ – input tensor;

$h_{i,j,k}^{(q)}$ – kernel.

For convenience, convolutional networks can be divided into groups, depending on what input data the neural network works with. In this paper we consider networks that receive input data in the form of a one–dimensional tensor (vector) and a two–dimensional tensor (matrix). In addition, the information from two receiving transformers is used to construct the input data representation.

II. Experimental Setup

The experimental setup is shown in Fig. 1 and is represented by personal workstation with a developed software, FPGA development board, fiber optic link, high frequency current transformers (HFCT), high–linear signal amplifier (AMP), and a unit under test (UUT). One of the DACs output of the development board is used for reference signal sending and is connected to air core transmitting HFCT–0 via AMP.

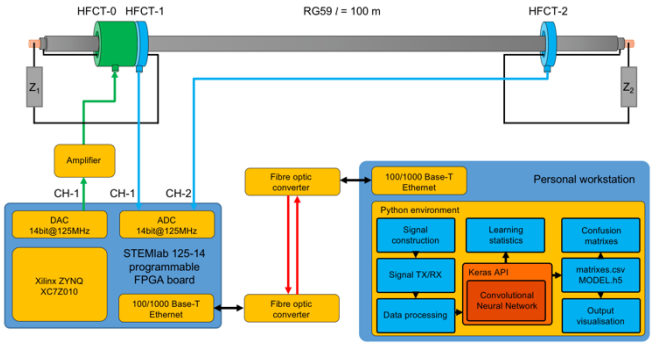

Fig. 1. The scheme of setup for reference signal sending and acquiring.

One of the ADCs input is used for receiving a sent signal, it is connected to HFCT–1, the other one is used for receiving a signal which passed through the coaxial cable (HFCT–2). Both receiving HFCTs have ferromagnetic cores. Impedances Z1 and Z2 are close to zero for this experiment. As an UUT we used a coaxial cable RG59, with a dielectric made of low–

This work was supported by the student research project SGS–2021–018.

978-1-6654-8082-6/22/$31.00 ©2022 IEEE

Authorized licensed use limited to: Univ of West Bohemia in Pilsen. Downloaded on October 24,2022 at 08:14:47 UTC from IEEE Xplore. Restrictions apply.

density polyethylene (LDPE). The UUT has been subjected to an accelerated thermal aging process. A total of 7 accelerated aging steps were carried out. Every accelerated aging step consists of the following procedures: thermal stress application; reference signal sending and acquiring; measuring of a partial discharges in a cable insulation. As a result, the following classes were obtained: Bt20–0, Bt100–12, Bt100–36, Bt100–72, Bt100–144, Bt100–288, Bt100–576. Where the letter "B" is the index of the cable in the experiment, the letter "t" stands for "thermal stress", indices 20 and 100 are the reference temperature (°C) of the cable and accelerated aging temperature (°C) of the cable respectively. The last index in the class name indicates cumulative duration of thermal stress in hours.

III. Reference Signal

Reference signal [4–7] has a length 130 sampled data points with the sampling period 8 ns. In this experiment, 18 variants of the reference signal were constructed and analyzed in two groups. The sweep start frequency for the first group, consisting of 9 variants, was 1 MHz, and the stop frequency was different for each variant and increased linearly in 1 MHz increments from 2 MHz to 10 MHz (Fig. 2). The sweep start frequency for the second group was 10 MHz, and the stop frequency was different for each variant and increased linearly in 1 MHz steps from 1 MHz to 9 MHz (Fig. 2). Every digitized raw signal record contains 16384 sampled values. Developed algorithm extracts useful part of the signal with a length 130 data points, simultaneously amplitude normalization and normalization in time–domain are applied [8].

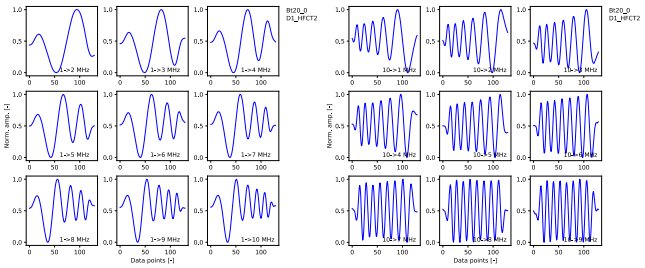

Fig. 2. Examples of 1–D reference signal representation (variant name is D1_HFCT2).

IV. Dataset

In this paper, 6 ways of signal preprocessing were designed and analyzed in order to identify the appropriate dimensionality of the neural network. The first way (named D1_HFCT2) uses only the signal from HFCT–2 as input to the neural network (Fig. 2). The second way also uses only the signal from HFCT–2, but this time not in the form of a time sequence, but in the form of a graphic file on which this sequence is depicted (D1_HFCT2_img). Therefore, for this type of signal representation we should use a two–dimensional convolutional neural network. The third way of representing the signal is also two–dimensional (Fig. 5), but in this case the image is constructed by placing both on the x–axis and y–axis the signal from HFCT–2, and it is projected on one of the axes with a small shift (D2_HFCT22), which gives a suitable distribution of the signal on the plane. The fourth method (Fig. 7) uses the difference of the signals received from HFCT–1 and HFCT–2 (D1_DIFF12), and the fifth method (D2_DIFF12_img) is a graphical representation of this difference, as in the case of method two. The sixth way (Fig. 10) builds a two-dimensional representation using signals from HFCT–1 and HFCT–2 (named D2_HFCT12).

V. Convolutional Neural Networks

In compiling the structure of the neural networks, we tried to maintain similarity for the one-dimensional and two-dimensional cases [9]. Both presented variants of the neural network (one-dimensional and two-dimensional) have two convolutional layers, which differ in their dimensionality. The first convolutional layer of the one-dimensional network has 8 filters with the dimensionality of kernels 3 (Tab. 1).

TABLE I. One-Dimensional Network Configuration

Layer	Parameters	Activation function
Conv1D	filters: 8; kernel size: 3	ReLU
Conv1D	filters: 16; kernel size: 3	ReLU
	Batch normalization	
Flatten		
Dense	Neurons: 128	ReLU
Dense	Neurons: 7	softmax

The second layer has 16 filters with kernels of dimensionality 3 as well. The first and second layers of the two-dimensional network have the same number of filters, but the dimensionality of the kernels in this case is 3 by 3 (Tab. 2). Another difference is the placement of a 2–by–2 pooling layer between the convolutional layers. The difference of one-dimensional structure is the use of Batch normalization function after the second layer [10]. The ReLU activation function was used for all layers except for the output layers. Softmax is used in the output layers. The number of neurons in the densely connected pre-output layers is 128, for both versions of neural networks – one–dimensional and two–dimensional.

TABLE II. Two-Dimensional Network Configuration

Layer	Parameters	Activation function
Conv2D	filters: 8; kernel size: (3, 3)	ReLU
MaxPooling	kernel size: (2, 2)	
Conv2D	filters: 16; kernel size: (3, 3)	ReLU
MaxPooling	kernel size: (2, 2)	
Flatten		
Dense	Neurons: 128	ReLU
Dense	Neurons: 7	softmax

VI. Results Discussion

Let's consider the variant of the one–dimensional neural network (Tab. 1), when time sequences obtained directly from HFCT–2 (Fig. 2) are fed to the neural network input. From the results of the classification (Fig. 3) for different frequencies of the reference signal, it can be seen that at frequencies up to 4 MHz, there is a consistently high level of correct classification. Basically, all degradation levels of the cable were determined here correctly, with 100 % result, and only in classes t1 and t2 the level of the correct classification fell down to 64 %. In the variants with higher stop frequencies, from 5 MHz to 10 MHz, in every case there is at least one level of degradation, where the percentage is very low. Consequently, at 1–8 MHz, the degradation level of t2 could not be recognized. Also, low percentage of correct results is

Authorized licensed use limited to: Univ of West Bohemia in Pilsen. Downloaded on October 24,2022 at 08:14:47 UTC from IEEE Xplore. Restrictions apply.

observed on variants t1 and t3. In the second group of reference signals, where the start frequency was equal to 10 MHz, we got very good results, the level of correctly identified signal samples only in one case (frequency 1–4 MHz, level t2) fell down to 88 %.

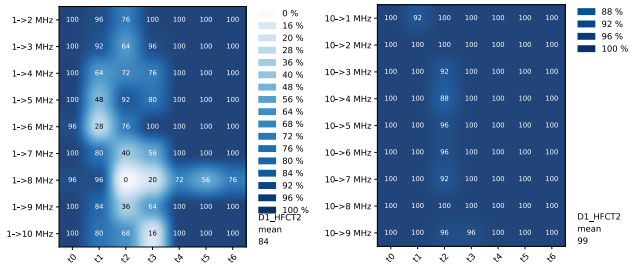

Fig. 3. Classification accuracy for variant D1_HFCT2.

Now, to compare the results of the one-dimensional network presented above with the results of the two–dimensional network, we will use the structure of the neural network given in Tab. 2. Since it is a two–dimensional neural network, it needs to be fed with appropriate data. To fulfil this, let's represent the previous signal not as a time sequence, but as a graphical file, on which this sequence is represented. As can be seen in Fig. 4, the classification results for the first group of reference signal have significantly improved. Now, only in one case the number of correctly recognized samples has fallen below 50% and amounted to 44 % (for the t2 variant at a frequency of 1–7 MHz). As for the second group of signals, no significant changes in the level of classification are observed here.

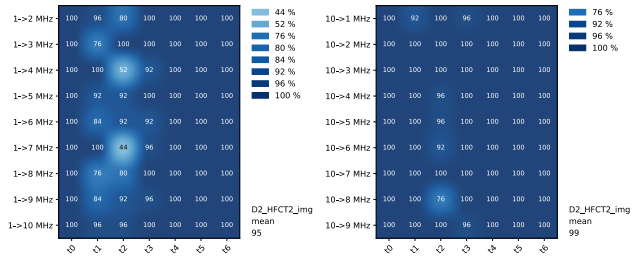

Fig. 4. Classification accuracy for variant D2_HFCT2_img.

Another way of representing the data is to build the graphical file using for x–axis and y–axis the data from HFCT–2. To obtain a suitable spatial distribution, a time shift of 48 ns was used when extracting the useful part of the signal from HFCT–2 data. Examples of images constructed in this way are shown in Fig. 5. Based on the results shown in Fig. 6, we can conclude that this method of data representation, in terms of the number of errors, is between the two previous variants.

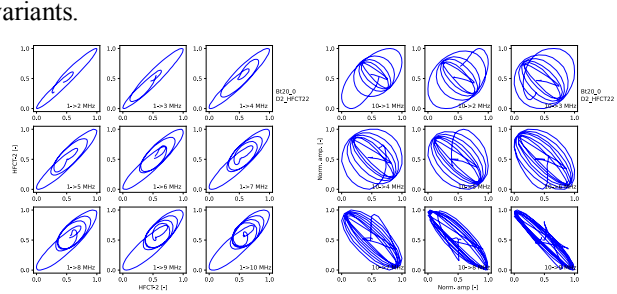

Fig. 5. Examples of 2–D refrence signal representation D2_HFCT22.

The important difference here is the presence of risk the neural network algorithm does not converge. In this case it happened for frequency 1–3 MHz and frequency 10–7 MHz. In variants D1_HFCT2 and D2_HFCT2_img such problem did not occur.

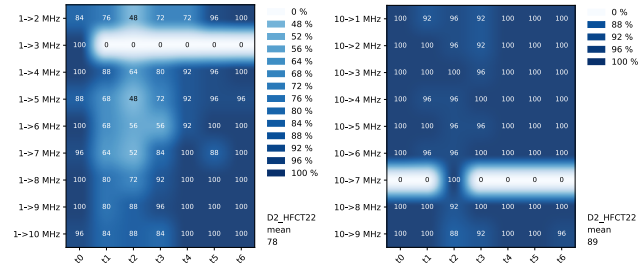

Fig. 6. Classification accuracy for variant D2_HFCT22.

To increase the level of data informative potential, next we will also use the signal coming from HFCT-2. For the case of a one-dimensional network, the construction of the input vectors will be done by subtracting the signal HFCT-1 from the signal received from HFCT-2. This process can also be seen as signal normalization, since in this case we feed the input of the network with data containing only the change in the signal that has passed through the cable. This version has been named D1_DIFF12, and examples of the signal are shown in Fig. 7.

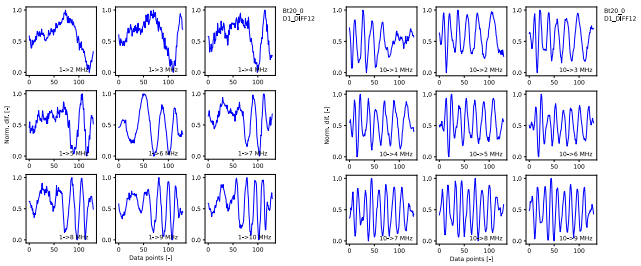

Fig. 7. Examples of 1–D refrence signal representation D1_DIFF12.

The result of the neural network is shown in Fig. 8. For the first group of frequencies, the error rate is about the same as for the first group of frequencies of the D1_HFCT2 variant, but here there is a decrease in the number of misclassifications as the frequency increases. With the second group of frequencies, all coaxial cable insulation degradation levels were determined to be 100 % correct. When using a two-dimensional network (D2_DIFF12_img variant), the classification accuracy (Fig. 9) decreases for the first group of frequencies. In the second group of frequencies there is a risk of missing the correct solution, as happened for 1–8 MHz.

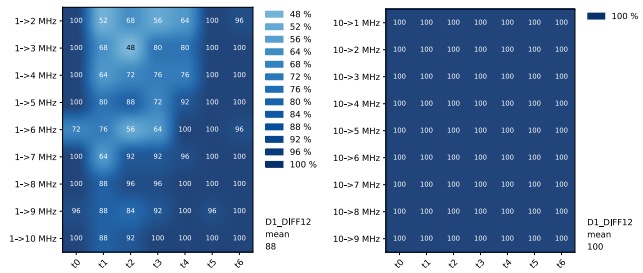

Fig. 8. Classification accuracy for variant D1_DIFF12.

Authorized licensed use limited to: Univ of West Bohemia in Pilsen. Downloaded on October 24,2022 at 08:14:47 UTC from IEEE Xplore. Restrictions apply.

The last variant studied in this experiment was D2_HFCT12 (Fig. 10). As can be seen from the abbreviation, this variant uses the signal from HFCT–2 on the x–axis and

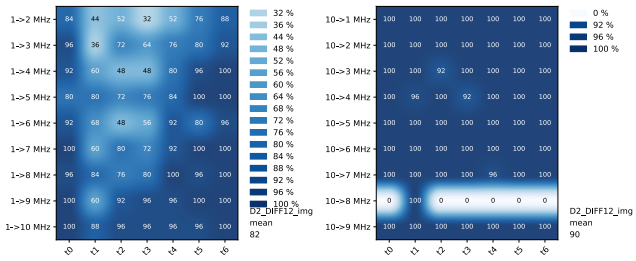

Fig. 9. Classification accuracy for variant D2_DIFF12_img.

the signal from HFCT–1 on the y-axis for the graphical representation. The results of the classification are shown in Fig. 11. The distribution pattern of the percentage of correct results is very similar to the D2_DIFF12_img variant. However, here in both frequency groups there are variants of frequencies where the algorithm was unable to perform training.

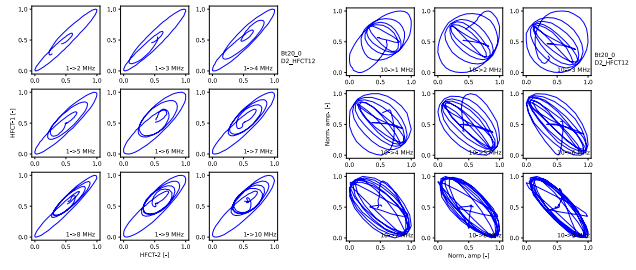

Fig. 10. Examples of 2–D refrence signal representation D2_HFCT12.

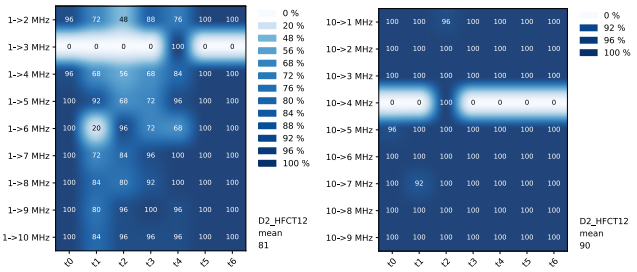

Fig. 11. Classification accuracy for variant D2_HFCT12.

VII. Conclusions

We can conclude that the use of a two–dimensional neural network is reasonable in the case where only the signal from one receiving transformer is used, in this case it is HFCT–2, since the classification accuracy in this case increases for the first group of frequencies. However, this applies only to the graphical representation of the one–dimensional signal. In the case when the result of subtracting the signals of two receiving transformers is used, the difference in the classification accuracy of degradation levels of accelerated thermal ageing of the coaxial cable insulation is not significant. In almost all variants in the first group the classification accuracy increases with increasing stop–frequency. Therefore, it is most advantageous to use variants of the reference signal with frequencies 1–8 MHz and above. In the second group of frequencies, the highest classification accuracy is observed. The variant of the dataset, where the result of subtracting the signals HFCT–1 and HFCT–2 was used, showed 100 % accuracy of the classification, using a one-dimensional neural network. The reference signal parameters from this set of frequencies are supposed to be used for further experiments. In general, this research showed that the one-dimensional neural network is the most suitable for this problem, and the result of subtraction of signals from two receiving high frequency current transformers (D1_DIFF12 variant) should be fed to the input of the neural network. And the most optimal reference signal is the signal from the second studied group, i.e. with a starting frequency of 10 MHz. In future work it is necessary to reveal the difference in computational resource consumption for the case of one–dimensional and two–dimensional neural networks.

References

[1] Liu, Manhua, Danni Cheng, and Weiwu Yan. “Classification of Alzheimer’s Disease by Combination of Convolutional and Recurrent Neural Networks Using FDG-Pet Images.” *Frontiers in Neuroinformatics* 12 (2018), doi: 10.3389/ fninf.2018.00035.

[2] Madrazo, Celia Fernández, Ignacio Heredia, Lara Lloret, and Jesús Marco de Lucas. “Application of a Convolutional Neural Network for Image Classification for the Analysis of Collisions in High Energy Physics.” *EPJ Web of Conferences* 214 (2019): 06017, doi: 10.1051/epjconf/201921406017.

[3] Nguyen, T.Q., Weitekamp, D., Anderson, D. *et al.* Topology Classification with Deep Learning to Improve Real-Time Event Selection at the LHC. *Comput Softw Big Sci* 3, 12 (2019), doi: 10.1007/s41781-019-0028-1.

[4] Y.-J. Shin et al., "Application of time-frequency domain reflectometry for detection and localization of a fault on a coaxial cable," in IEEE Transactions on Instrumentation and Measurement, vol. 54, no. 6, pp. 2493-2500, Dec. 2005, doi: 10.1109/TIM.2005.858115.

[5] G.-Y. Kwon et al., "Offline Fault Localization Technique on HVDC Submarine Cable via Time–Frequency Domain Reflectometry," in IEEE Transactions on Power Delivery, vol. 32, no. 3, pp. 1626-1635, June 2017, doi: 10.1109/TPWRD.2017.2680459.

[6] C.-K. Lee, S. J. Chang, M. K. Jung and Y.-J. Shin, "Condition monitoring of cable aging via time-frequency domain reflectometry in real-time," 2017 IEEE Conference on Electrical Insulation and Dielectric Phenomenon (CEIDP), 2017, pp. 290-294, doi: 10.1109/CEIDP.2017.8257585.

[7] C. -K. Lee et al., "Real-Time Condition Monitoring of LOCA via Time–Frequency Domain Reflectometry," in IEEE Transactions on Instrumentation and Measurement, vol. 66, no. 7, pp. 1864-1873, July 2017, doi: 10.1109/TIM.2017.2664578.

[8] M. Olkhovskiy, E. Müllerová and P. Martínek, "Reference Signal Processing for Aging State Recognition," *2021 International Conference on Applied Electronics (AE)*, 2021, pp. 1-4, doi: 10.23919/AE51540.2021.9542898.

[9] P. Y. Simard, D. Steinkraus and J. C. Platt, "Best practices for convolutional neural networks applied to visual document analysis," Seventh International Conference on Document Analysis and Recognition, 2003. Proceedings., 2003, pp. 958-963, doi: 10.1109/ICDAR.2003.1227801.

[10] A. Kumar, "Effects of Different Normalization Techniques on the Convolutional Neural Network," *2021 8th International Conference on Computing for Sustainable Global Development (INDIACom)*, 2021, pp. 201-204, doi: 10.1109/INDIACom51348.2021.00036.

Authorized licensed use limited to: Univ of West Bohemia in Pilsen. Downloaded on October 24,2022 at 08:14:47 UTC from IEEE Xplore. Restrictions apply.